Model-Based Synthetic Fuzzy Logic Controller for Indirect Blood Pressure Measurement

Jia-Jung Wang, Chin-Teng Lin, *Senior Member, IEEE*, Shing-Hong Liu, and Zu-Chi Wen

***Abstract*—In this paper, a new measurement system for the noninvasive monitoring of the continuous blood pressure waveform in the radial artery is presented. The proposed system comprises a model-based fuzzy logic controller, an arterial tonometer and a micro syringe device. The flexible diaphragm tonometer is to register the continuous blood pressure waveform. To obtain accurate measurement without distortion, the tonometer's mean chamber pressure must be kept equal to the mean arterial pressure (MAP), the so-called *optimal coupling condition*, such that the arterial vessel has the maximum compliance. Since the MAP cannot be measured directly, to keep the optimal coupling condition becomes a tracking control problem with unknown desired trajectory. To solve this dilemma, a model-based fuzzy logic controller is designed to compensate the change of MAP by applying a counter pressure on the tonometer chamber through the micro syringe device. The proposed controller consists of a model-based predictor and a synthetic fuzzy logic controller (SFLC). The model-based predictor is to estimate the MAPs changing tendency based on the identified arterial pressure-volume model. The SFLC is composed of three subcontrollers, each of which is a simple fuzzy logic controller, for processing the three changing states of the MAP: ascending, descending and stabilizing states, respectively. Simulation results show that, for the MAP with changing rates of ±10, ±20 or ±30 mm Hg/min, the model-based SFLC can beat-to-beat adjust the tonometer's chamber pressure only with a mean square error of 1.9, 2.2, or 2.8 mm Hg, respectively.**

***Index Terms*—Compliance, fuzzy logic control, mean arterial pressure, oscillometry, tonometer.**

I. INTRODUCTION

THE current technologies of indirect blood pressure measurement primarily include the oscillometric and Korotkoff methods. Both methods apply an occlusive cuff, as an external pressure source, wrapping around a subject's upper arm to disclose the systolic and diastolic pressures within 30 to 60 s. In the oscillometric method, as the occluding cuff pressure is gradually reduced from above systolic values to below diastolic values, occlusive cuff pressure oscillations show a specific pattern [6], [10], [29]. It is now generally accepted that *a maximum vessel volume pulse or occlusive cuff pressure oscillation occurs when the occlusive cuff pressure is identical to the mean arterial pressure (MAP)* [2], [3], [7]. This means that the artery can be considered to be in an *optimal coupling condition* between the artery and the cuff pressure.

A number of techniques have been proposed to noninvasively detect continuous arterial blood pressure waveform [12], [21], [32]. Yamakoshi and others employed the vascular unloading technique to measure the continuous blood pressure from the arteries in fingers and heads [27], [36]. In their instruments, the cuff pressure is set up only in the beginning at the level of a subject's MAP. Since Stein and Blick first developed a mechanical force-sensing arterial tonometer, various kinds of tonometers using piezoelectric crystals have been designed to register the blood pressure waveform in the superficial artery [9], [26], [33], [39]. However, only a moderate accuracy was achieved when applying those tonometers. By means of registering the radial artery filling, the rapid noninvasive measurement of arterial opening pressure was performed with a photoplethysmography [25]. Drzewiecki *et al.* designed a flexible diaphragm tonometer to simultaneously measure arterial blood pressure waveform and vessel volume pulse [8]. Because these studies usually did not consider the coupling condition between the sensor and the artery, the accuracy of the measured blood pressure waveform with their devices was uncertain due to not taking the time-varying MAP into account.

Several control techniques have been proposed in the drug syringe to remain the patient's MAP in the desired range [4], [16], [22]. These control schemes can be classified as set-point control schemes, in which the plant has a target output for determining the error signal for the controller. Moreover, most of the previous control systems operated mainly on mathematical models of patients. However, it is difficult to identify a useful and simple mathematical model of patients due to the complexity of the human body. Even with an available mathematical model, it is still not easy to design a controller to meet the practical requirements. Recently, fuzzy logic control (FLC) has been widely applied in the anesthesia control and other biomedical control [14], [20], [31]. One of the advantages in using the FLC is that it can be constructed empirically without explicit mathematical models of nonlinear physiological systems.

The goal of this paper is to design a system for measuring the continuous blood pressure waveform accurately without distortion. In order to achieve this goal, we use a modified flexible diaphragm tonometer to sense the continuous blood pressure waveform through a pressure transducer [30]. Importantly, in the measuring process, we should keep the tonometer's mean chamber pressure equal to the MAP, i.e., to keep the

Manuscript received June 6, 2001; revised September 11, 2001 and December 27, 2001. This work was supported by the National Science Council of Taiwan, R.O.C., under Grant NSC 90-2213-E–009-103. This paper was recommended by Associate Editor W. Pedrycz.

J.-J. Wang is with the Department of Biomedical Engineering, I-Shou University, Kaohsiung, Taiwan, R.O.C.

C.-T. Lin is with the Department of Electrical and Control Engineering, National Chiao-Tung University, Hsinchu 300, Taiwan, R.O.C. (e-mail: ctlin@fnn.cn.nctu.edu.tw).

S.-H. Liu is with the Department of Biomedical Engineering, Yuanpei Institute of Science and Technology, Hsinchu 300, Taiwan, R.O.C.

Z.-C. Wen is with the Hsinchu Hospital, Department of Health Executive Yuan, Hsinchu 300, Taiwan, R.O.C.

Publisher Item Identifier S 1083-4419(02)03004-2.

optimal coupling condition, such that the chamber pressure can accurately reflect the intra-arterial blood pressure waveform without distortion, because the arterial vessel has the maximum compliance in this condition [7], [11], [23], [28]. However, since the MAP cannot be measured directly, it is difficult to design a controller to make the tonometer's mean chamber pressure to track the MAP directly. As a result, we shall apply the *oscillometric principle* which indicates that if the detected vessel volume pulse can be kept at its maximum amplitude, the optimal coupling condition can be guaranteed [34], [35]. According to this principle, since the vessel volume pulse can be measured by the tonometer through the impedance method, the control objective in our measuring system is to keep the vessel volume pulse always at its maximum amplitude. However, the relationship between the amplitude of the detected vessel volume pulse and the difference of the mean chamber pressure and the MAP (i.e., the *transmural* pressure) is nonmonotonous Gaussian-function-typed. Moreover, since the MAP always responses to human physiological conditions, it varies with time. Hence, when the detected vessel volume pulse departs from the maximum amplitude, the controller has no sense on the adjustment direction. Therefore, to maintain the optimal coupling condition is a time-varying trajectory-tracking control problem with unmeasureable desired trajectory for tracking [18], which is a challenging task. To solve this problem, a predictor is designed to estimate the changing tendency of the MAP. When the estimated MAP is increasing, the controller should increase the chamber pressure; otherwise, the controller should decrease the chamber pressure such that the vessel volume pulse can regain its maximum value. In this way, the optimal coupling condition can be maintained stably.

According to the approach described in the above, the proposed system for measuring the arterial blood pressure waveform contains a fuzzy controller, a model-based predictor, a modified tonometer and a micro syringe device. The tonometer can simultaneously register the arterial blood pressure waveform and vessel volume pulse and thus, through the micro syringe device, the changed vessel volume amplitude induced by the change of the MAP can be compensated by applying a counter pressure to maintain the maximum vessel volume amplitude. A proposed synthetic fuzzy logic controller (SFLC) is utilized to control the micro syringe. The SFLC is composed of three parallel subcontrollers, each of which is a simple fuzzy logic controller, for processing the three changing states of the MAP: ascending, descending and stabilizing states, respectively. At the same time, a model-based predictor is utilized to estimate the MAPs changing tendency and suitably trigger one of the three subcontrollers.

In order to construct a more reliable simulation environment, the arterial blood pressure waveform and vessel volume pulse are simultaneously measured with the modified tonometer for nine subjects. Based on the experimental data, we derive a static arterial pressure-volume relationship as a target model in the noninvasive blood pressure measurement. Then we use this model as the plant of the proposed measurement system and to construct a model-based predictor. Under different changing rates of the MAP, the simulated results show the good estimation capability of the model-based predictor that can estimate the tendency of MAP and adapt the SFLC well. The SFLC can successfully control the mean chamber pressure of the tonometer to achieve the optimal coupling condition in the measuring process.

This paper is organized as follows. In Section II, the sensory device and the chamber-artery model are described. In Section III, the model-based synthetic fuzzy logic controller is designed for the proposed measuring system. In Section IV, the experimental process for modeling and the simulation results of the chamber pressure control based on the proposed measurement system using the model-based SFLC are presented. Conclusions are made in Section V.

II. Sensory Device and Chamber-Artery Model

In this section, we design the noninvasive measurement system to record the continuous arterial blood pressure waveform based on a modified tonometer. In order to get the accurate blood pressure waveform, this system must keep the tonometer's mean chamber pressure equal to the MAP, i.e., to keep the optimal coupling condition. However, since the MAP cannot be measured directly, we shall take use of the oscillometric principle, which indicates that if the detected vessel volume pulse can be kept at its maximum amplitude, the optimal coupling condition can be guaranteed. Therefore, we modify a tonometer such that it not only can measure the arterial blood pressure waveform by a pressure transducer but also can detect the vessel volume pulse through the impedance method simultaneously. We also design a micro syringe device to change the chamber pressure of the tonometer to track the MAP. Based on this measurement device, we then apply the oscillometric principle to derive a Gaussion-function-type model for modeling the static arterial pressure-volume relationship under the tonometer.

A. Structure and Principle of the Tonometer

A flexible diaphragm arterial tonometer, modified from the previous studies is constructed to detect the arterial blood pressure and the vessel volume pulse simultaneouly [8], [23]. The tonometer is made principally of plexiglass and is miniaturized so that it could be directly positioned over a superficial artery. As shown in Fig. 1, inside the tonometer is a hollow chamber into which users can perfuse saline. Within the chamber are four electrodes, made of stainless steel, that are arranged in parallel. There are two fluid outlets in the tonometer: one is for the filling of the chamber and the other is for the removal of the air in the saline if present.

The change in the chamber pressure is continuously monitored using a pressure transducer (NPI-12, Lucas, USA) that is connected to the chamber. To reduce the distortion of the pressure waveform caused during transmission, the distance between the sensor and the chamber is kept as short as possible. Also, the connecting tube between them is made from stiffer material.

In the study, the variation of the vessel volume is assessed using the impedance plethysmography [8]. In this method, a constant current source is designed and connected to any two of electrodes. As the current passed through the conductive fluid

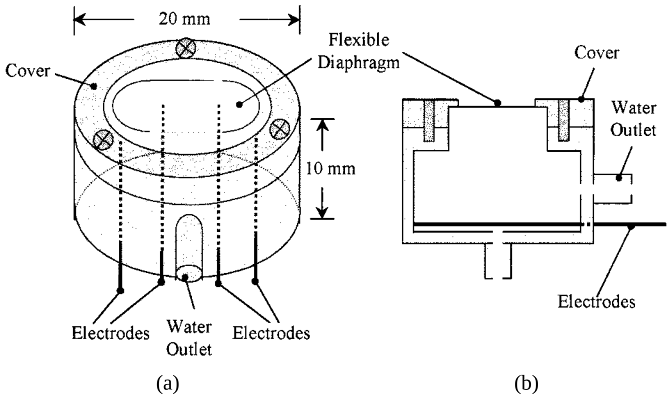

Fig. 1. (a) Three-dimensional view of the modified flexible diaphragm arterial tonometer and (b) sectional view of the flexible diaphragm tonometer.

(here, saline) between the two electrodes, a voltage difference is induced between them.

The resistance, R, of a rectangular compartment, corresponding to the space between the two electrodes, can be represented by

$$R = \frac{\rho L}{A} \tag{1}$$

where ρ is the resistivity of the fluid in the compartment, L is the length and A is the cross-section area of the compartment. Based on the fact that the volume of the compartment, V_{cpt}, is the product of L and A, the resistance can be expressed as

$$R = \frac{\rho L^2}{V_{cpt}}. \tag{2}$$

Then, the voltage difference, V_{vd}, across the compartment can be obtained by

$$V_{vd} = IR = \frac{\rho I L^2}{V_{cpt}} \tag{3}$$

where I is the current passing through the compartment.

From (3), it is clear that V_{cd} is inversely proportional to the compartment volume. That is, as ρ and L are maintained and a constant current is applied, the more the volume, the smaller the voltage difference between the two electrodes.

B. Micro Syringe Device

Fig. 2 shows the structure of the micro syringe device. This device includes a stepping motor (TECO, Taiwan), a self-designed spiral stick and a micro syringe (500F-LL-GT, GAS, USA). When the predictor detects a change in the MAP, the stepping motor is triggered by the controller to push or pull the micro syringe so as to increase or decrease the amount of saline in the tonometer chamber. This will then result in an increment or decrement of the chamber pressure directly.

C. Modeling of Tonometer Chamber

With the flexible diaphragm tonometer, sensing the fluctuation in the chamber fluid pressure of the tonometer may indirectly assess the arterial blood pressure in this study. This measurement is based on a principle known as the indirect vascular

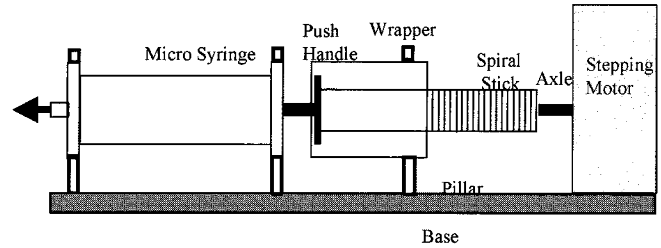

Fig. 2. Structure description of the micro syringe device.

unload which was proposed in the oscillometry [13], [34]. Generally, previous investigators concluded that when the vessel volume pulse or occlusive cuff pressure oscillation arrived at its the maximum amplitude, the occlusive cuff pressure was nearly equal to the MAP.

Here, for convenience, it is assumed that the overall arterial mechanical properties can be dominated by a static arterial pressure-volume relationship [2], [24]. This is depicted by

$$V_{vol} = \begin{cases} V(t)e^{aP_t}, & \text{if} \quad P_t \leq 0 \\ V_{\max} + (V(t) - V_{\max})\, e^{bP_t}, & \text{if} \quad P_t > 0 \end{cases} \tag{4}$$

where V_{vol} is the vessel volume at the P_t, $V(t)$ is a simulated waveform of vessel volume, $V_{\max}$ is the vessel volume when the artery is fully expanded, both a and b are constants, and P_t is the transmural pressure which is equal to the difference between the MAP and the chamber pressure P_c as

$$P_t = MAP - P_c. \tag{5}$$

This waveform of vessel volume is synthesized using a Fourier series representation

$$V(t) = V_{dc} + A_0 \sin\left(\frac{2\pi f_{hr}}{60}\right) + A_1 \sin\left(\frac{4\pi f_{hr}}{60} + \phi\right) \tag{6}$$

where f_{hr} is the heart rate and V_{dc}, A_0 and A_1 are constant values, ϕ is the phase. One typical representation of this relationship is described in Fig. 3, assuming the MAP is 90 mm Hg. With an inflation rate of 3 mm Hg/min, Fig. 3(a) describes the oscillation curve, showing the relationship of the vessel volume pulses to the chamber pressure. During the period of inflation, the amplitude of the oscillation is gradually augmented and then declines and arrives at its maximum as the chamber pressure is around the MAP. Fig. 3(b) shows the distribution of the local maximums of the vessel volume pulses in the oscillation curve versus the chamber pressure.

By the curve fitting techniques [17], the envelope of the vessel volume oscillation amplitude, VOA, can be approximated by a Gaussian curve represented by the solid line in Fig. 3(b). This can be represented by

$$VOA = VOA\max e^{-0.5((Pc-MAP)/\sigma)^2} \tag{7}$$

where σ is a constant and $VOA\max$ is the maximum of VOA.

III. Model-Based Synthetic Fuzzy Logic Control

In normal control process, the difference between the measured output and the desired output is used as feedback to the

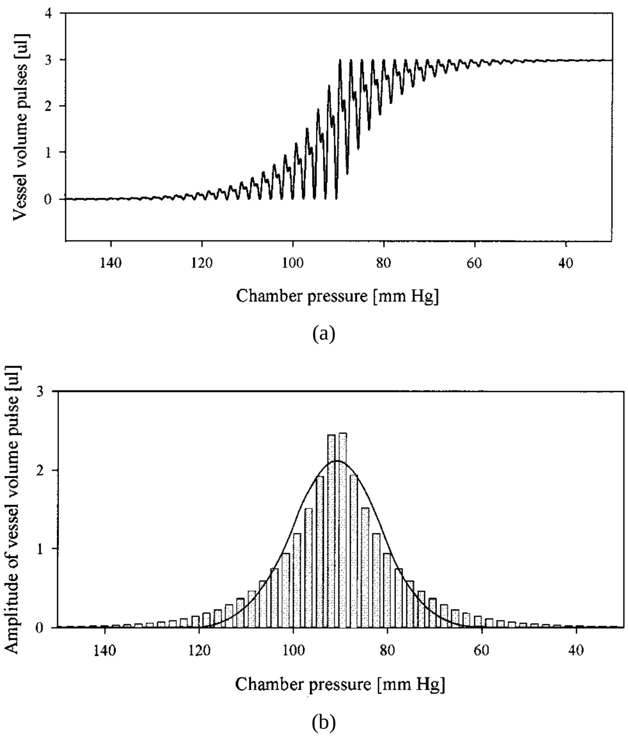

Fig. 3. Static arterial pressure-volume relationship from the mathematical derivations in (5)–(7). (a) Vessel volume pulse versus chamber pressure and (b) amplitude of vessel volume pulse versus chamber pressure. The curve is obtained by setting $V\max = 3\ \mu$l, $a = -0.1$ mm Hg-1 and $b = 0.1$ mm Hg-1, assuming that the vessel volume is in a simulated waveform, the heart rate is 85 beats/min (bpm) and the MAP is 90 mm Hg.

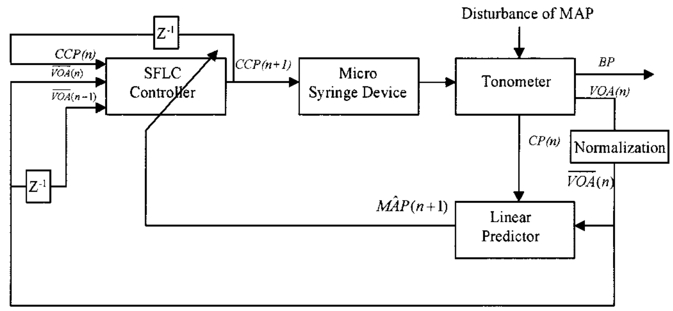

Fig. 4. Block diagram of the closed-loop chamber pressure control of the proposed measurement system.

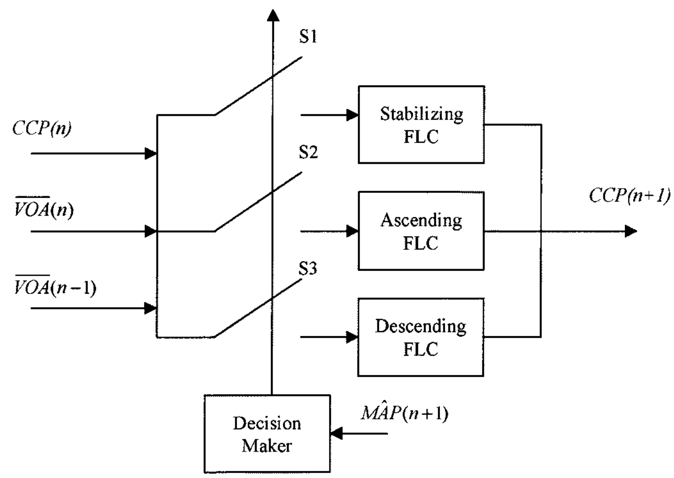

Fig. 5. Structure of the proposed SFLC that includes the ascending, descending and stabilizing subcontrollers and decision maker.

controller, controlling the plant to achieve the level of the desired output [14], [18], [38], the so-called "set-point control." According to the oscillometric principle and the optimal coupling condition described in Section II, since the vessel volume pulse can be measured by the tonometer, the aim of our controller is to keep the vessel volume pulse at its maximum amplitude. An obvious dilemma of this control goal is that the maximum amplitude to be approached is *changing from time to time and is unknown in advance*. Hence, what we encounter is a time-varying trajectory tracking control problem with unknown desired trajectory. If the chamber pressure is greater or lower than the apparent MAP, the amplitude of vessel volume pulse will become smaller than the maximum, as shown in Fig. 3. In addition, since how the subject's MAP varies with time and whether the MAP is in the ascending or descending state are unknown, the controller cannot utilize the difference information to adjust the chamber pressure. Therefore, the model-based SFLC is implemented in this section to deal with this problem. The model-based SFLC consists of the SFLC and a model-based predictor of MAP tendency. The SFLC can control the measurement system under three different states of the MAP and the model-based predictor can estimate the MAPs changing tendency to regulate the SFLC appropriately.

A. Synthetic Fuzzy Logic Controller

The block diagram of the close-loop chamber pressure control system of the proposed measurement system is shown in Fig. 4. The entire system comprises a SFLC, a model-based predictor used to adjust the SFLC, a micro syringe device used to change the chamber pressure of the tonometer and proper disturbance added to the simulation model to create a more realistic control environment. It is likely that a great change in MAP (ascending or descending) occurs due to blood pressure-related diseases or other intervention. In accordance with this phenomenon, the proposed SFLC is composed of three parallel subcontrollers, i.e., the Stabilizing, Ascending, and Descending FLCs, as shown in Fig. 5. A decision maker designates one of the three subcontrollers to operate based on the estimation result of the model-based predictor that is used to beat-to-beat evaluate the changing tendency of MAP. In the beginning, because the tonometer only detects the blood pressure waveform, we need using an oscillometric method to measure the MAP, systolic and diastolic pressures. Then, the measurement system triggers the micro syringe device to make the chamber equal to the MAP and uses the systolic and diastolic pressures to calibrate the blood pressure waveform. This finishes the initialization step of our system before the adaptive control of the SFLC. After this initialization step, the SFLC begins to adapt the chamber pressure following the MAP. Hence, for $n = 0$, $CCP = 0$ and VOA is its maximum $VOA\max$ when the chamber pressure is equal to MAP. The SFLC designed here requires three input variables, including the current and preceding normalized oscillation amplitude of vessel volume, $\overline{VOA}(n)$ and $\overline{VOA}(n-1)$ and the amount of change in the chamber pressure, $CCP(n)$. The output of the SFLC, $CCP(n+1)$, is used to trigger the micro syringe device, regulating the chamber pressure. Here,

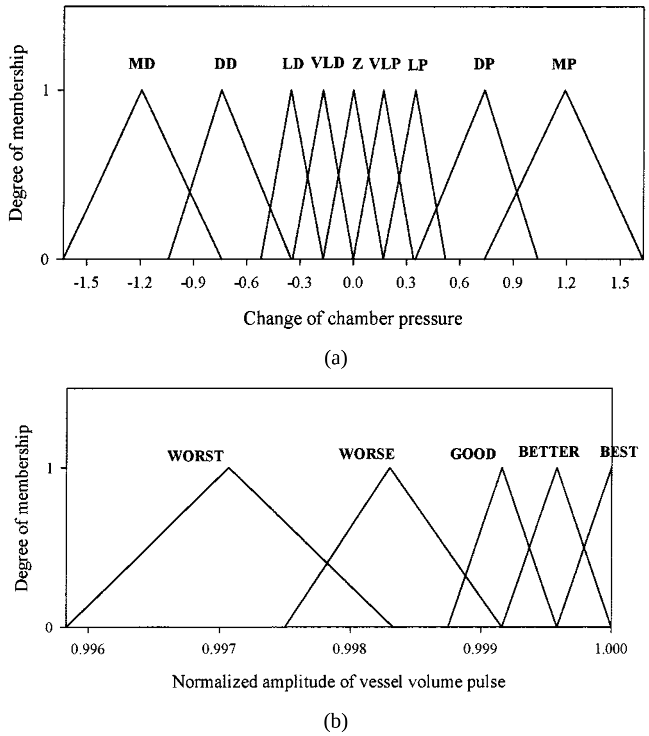

Fig. 6. Fuzzy term sets for the ascending and descending FLCs. (a) The nine membership functions of the change in the chamber pressure, $CCP(n)$: "MP," "DP," "LP," "VLP," "Z," "VLD," "LD," "DD," and "MD." (b) The five membership functions of the normalized amplitudes of the vessel volume pulse, $\overline{VOA}(n)$ or $\overline{VOA}(n-1)$: "BEST," "BETTER," "GOOD," "WORSE," and "WORST."

$n-1$ and $n+1$ indicate the preceding and the next sampling time of n, respectively [19], [37].

The three parallel subcontrollers possess the similar fuzzifiers and defuzzifiers, but have different rule bases. In either of the Ascending and Descending FLCs, the fuzzy term set for $CCP(n)$ is composed of nine membership functions [Fig. 6(a)]: much push (MP), moderately push (DP), little push (LP), very little push (VLP), zero (Z), very little draw (VLD), little draw (LD), moderately draw (DD), and much draw (MD). These fuzzy terms are defined by means of triangular functions in the [−1.63 1.63] subset of real numbers. As shown in Fig. 6(b), the normalized oscillation amplitude of vessel volume, $\overline{VOA}(n)$ or $\overline{VOA}(n-1)$, determine the degree of the coupling between the vessel's side and the tonometer's side with five membership functions, defined in the [0.9942 1] subset of real numbers: BEST, BETTER, GOOD, WORSE, and WORST. In the Stabilizing FLC, the fuzzy terms of $CCP(n)$ are defined in [−1.12 1.12] and those of $\overline{VOA}(n)$ and $\overline{VOA}(n-1)$ are defined in [0.9924 1].

In designing fuzzy rules, we followed these concepts. If $\overline{VOA}(n)$ is worse than $\overline{VOA}(n-1)$ and $CCP(n)$ is VLP in the ascending state, $CCP(n+1)$ will be LP to elevate the more chamber pressure. Since the Ascending FLC is activated by the decision maker when the MAP is in the ascending state, i.e., in the direction of approaching its maximum. On the contrary, if $\overline{VOA}(n)$ is worse than $\overline{VOA}(n-1)$ and $CCP(n)$ is VLD in the descending state, $CCP(n+1)$ will be LD to decrease the more chamber pressure. Since the Descending FLC is activated when the MAP is in the descending state, i.e., in the direction of departing from its maximum. Therefore, the functions of the rules of the Ascending FLC are opposite to those of the Descending FLC. In the Stabilizing FLC, if $\overline{VOA}(n)$ is worse than $\overline{VOA}(n-1)$ and $CCP(n)$ is VLP, then this control action is incorrect. Thus, $CCP(n+1)$ will be LD to reduce the chamber pressure at the next time step, $n+1$. Fundamentally, the rule structure of the Stabilizing FLC is itself symmetric.

The individual-rule-based inference process is supervised by computing the degree of match between the fuzzified input values and the fuzzy set describing the meaning of the rule-antecedent, as described in the rule set [5]. As expressed in (8), shown at the bottom of the page, the output μ is produced by clipping the fuzzy membership functions and the possibility distribution function is then found by applying the Mamdani's max-min operator, where inputs are $\mu = \overline{VOA}(n)$, $v = \overline{VOA}(n-1)$ and $y = CCP(n)$ and output is $w = CCP(n+1)$, where n is fire rules number. The technique of "center of gravity" is used to process the defuzzification and to calculate the output, $CCP(n+1)$, of the controllers, as expressed

$$CCP(n+1) = \frac{\sum_{j=1}^{m} \mu_{CCP(n+1)}(z_j) z_j}{\sum_{j=1}^{m} \mu_{CCP(n+1)} z_j} \tag{9}$$

where m is the number of quantization levels of the output, z_j is the amount of degree output at the quantization level j and $\mu_{CCP(n+1)}(z_j)$ represents its membership value in the output fuzzy set $CCP(n+1)$.

B. Model-Based Predictor of Mean Arterial Pressure Tendency

In the previous section, we derived the tonometer chamber-artery model (7). This model is used here to identify the varying situations of the MAP. The goal is to predict the changing tendency of the MAP, i.e., to identify whether the MAP is in ascending, stabilization, or descending state. To achieve this goal, we shall design a linear predictor to predict the value of MAP at the k_{th} time step, $M\hat{A}P_k$, such that the difference between the corresponding $V\hat{O}A_k$ and the real VOA_k is minimum [1]. In other words, the least square criterion for tuning the linear predictor based on the k_{th} sample is

$$E_k\left(M\hat{A}P_k\right) = \left[VOA_k - V\hat{O}A_k\right]^2 = \varepsilon_k^2\left(M\hat{A}P_k\right) \tag{10}$$

where from (7), $VOA_k = VOA\max, ke^{-0.5((P_{c,k}-MAP_k)/\sigma)^2}$ is the real vessel volume amplitude, $V\hat{O}A_k = VOA\max, ke^{-0.5((P_{c,k}-M\hat{A}P_k)/\sigma)^2}$ is the estimated amplitude when the

$$\mu_{CCP(n+1)}(w) \equiv \bigvee_{i}^{n} \left\{ \left[\mu_{\overline{VOA}(n)_i}(u) \wedge \mu_{\overline{VOA}(n-1)_i}(v) \wedge \mu_{CCP(n)_i(y)} \right] \wedge \mu_{CCP(n+1)_i}(w) \right\} \tag{8}$$

parameter is $M\hat{A}P_k$, $\varepsilon_k = (VOA_k - V\hat{O}A_k)$ is the prediction error, where $VOA_{\max,k}$ is the maximum of VOA_k, $P_{c,k}$ is the chamber pressure at time k, MAP_k is the real MAP at time k. The least square criterion aims at minimizing (10), by taking the gradient of the optimization criterion:

$$\frac{\partial E_k\left(M\hat{A}P_k\right)}{\partial M\hat{A}P_k} = \frac{2}{\sigma}\varepsilon_k V\hat{O}A_k\left(P_{c,k} - M\hat{A}P_k\right). \quad (11)$$

Therefore, the recursive linear predictor using the gradient is described by

$$M\hat{A}P_{k+1} = M\hat{A}P_k + \frac{g}{\sigma}\varepsilon_k V\hat{O}A_k\left(P_{c,k} - M\hat{A}P_k\right) \quad (12)$$

where g is the constant gain. Here, we use the gradient of $M\hat{A}P_k$ as the decision value. If a decision value falls within a threshold region, it means that the present MAP is in a stable state. Thus, the decision maker will trigger the Stabilizing FLC of the SFLC to keep the chamber pressure. However, if a decision value is beyond the threshold region, it implies that the MAP is ascending or descending now, so the decision maker will activate either the Ascending FLC or Descending FLC of the SFLC.

IV. Experiment and Simulation Results

A. Experimental Process

Nine subjects (two females and seven males, 18 ~ 37 years) with normotension were enrolled to assess the static relationship of the vessel volume amplitude to the transmural pressure. Each subject's blood pressure waveform and vessel volume pulse in sitting position were simultaneously measured with the modified tonometer that was placed over the radial artery of the subject and fixed with an elastic bandage. The chamber pressure of the tonometer was gradually increased up to 160 mm Hg, at a rate of 3 mm Hg/s by means of the controlled micro syringe device. A period of about 30-second original measured signal of the chamber pressure and vessel volume pulse for each subject was digitized with a sampling frequency of 200 Hz and recorded using the MP 100 Manager (BIOPAC System, Inc., USA). Analysis of the arterial pressure-volume relationship was performed using a software package offered by SigmaPlot (SPSS, Inc., USA).

B. Simulation Results and Performance Comparisons

Before undergoing the experiment, the nine subjects' systolic (120 ± 11 mm Hg) and diastolic (71 ± 9 mm Hg) pressures were measured using an automatic blood pressure monitor (OMRON R3, Japan). Their corresponding MAPs were approximately assessed by summing two thirds of the systolic pressure and one third of the diastolic pressure and found to be 87 ± 8 mm Hg. Fig. 7 shows the static arterial pressure-volume relationships obtained using one typical recording from the nine subjects. Fig. 7(a) shows the curve of the vessel volume pulses yielded by high-pass filtering the original measured signal of vessel volume. All amplitudes of the vessel volume pulses corresponding to each heartbeat are extracted and plotted with respect to the transmural pressure, as shown in Fig. 7(b). It can be seen

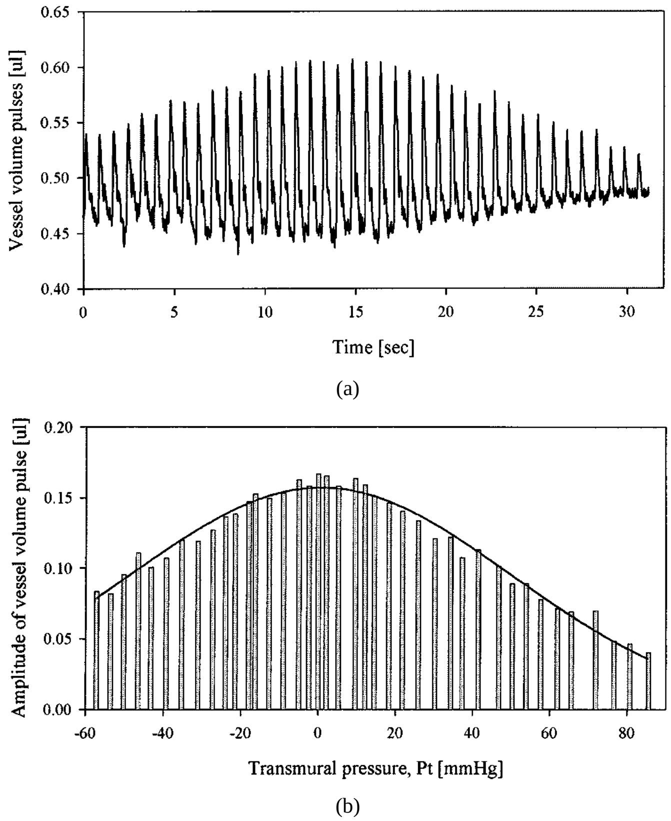

Fig. 7. Derivation of the static arterial pressure-volume relationship from subject no. 1. (a) Curve of vessel volume pulse versus the chamber pressure and (b) distribution of the maximum vessel volume amplitude with respect to the chamber pressure.

TABLE I
SUMMARY OF REGRESSION PARAMETERS FOR THE GAUSSIAN FUNCTION AND THE VALUES OF BLOODPRESSURE FOR NINE SUBJECTS

Subject	R	SEE	σ [mm Hg]	SYS [mm Hg]	DIS [mm Hg]	MAP [mm Hg]	Sex
1	0.987	0.0059	49.3	128	83	95	Male
2	0.896	0.0168	45.1	126	65	85	Male
3	0.921	0.0195	59.2	121	64	83	Male
4	0.888	0.0163	35.8	95	56	69	Female
5	0.889	0.0222	39.4	123	74	90	Male
6	0.924	0.0106	30.9	112	72	85	Female
7	0.813	0.0193	45	126	75	92	Male
8	0.948	0.0077	29.1	128	65	86	Male
9	0.932	0.0092	31.5	122	81	95	Male
Mean	0.911	0.014	40.6	120	71	87	
± SD	0.048	0.006	9.9	11	9	8	

that a peak occurs when the chamber pressure is equal to the MAP. Also shown is the curve-fitting result using the Gaussian function (solid line). In Table I, we list the values of the regression parameters for Gaussian function and the values of blood pressure for each subject, including the regression (R), the standard error of estimate (SEE), the parameter σ in (7), the systolic pressure (SYS), the diastolic pressure (DIS), the mean arterial pressure (MAP) and the sex of subjects. In the table, we also show the mean and the standard deviation (SD) of each parameter. Notice that the values of the parameter σ corresponding to the nine subjects' models are very distinct and their mean is 40.6 mm Hg.

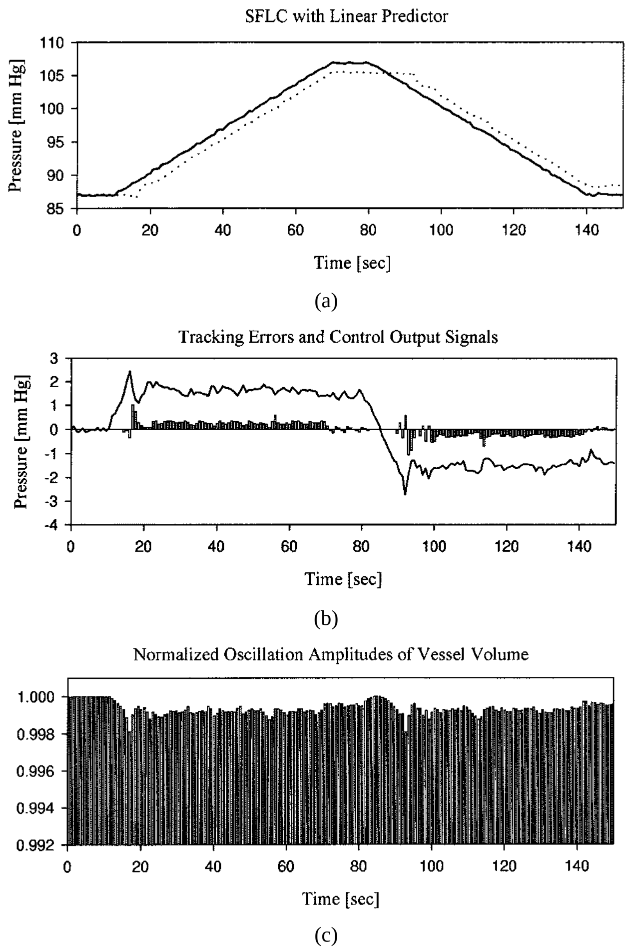

Fig. 8. Simulation results of the SFLC with a model-based linear predictor for the MAP with a changing rate of ± 20 mm Hg/min. (a) The desired MAP (solid line) and the chamber pressure (CP) under control (dot line), (b) the difference between the desired MAP and the chamber pressure (solid line) and the SFLCs output signals (bar lines), and (c) the normalized oscillation amplitude of vessel volume in each heartbeat.

We modeled the arterial pressure-volume relationship by (7), in which the value $VOA\max$ is 1, the σ is 40.6 mm Hg and the MAP is 87 mm Hg. In order to test the generalization capability of the SFLC, the chamber pressure was controlled to follow one of the three desired MAPs changing rates, including ± 10, ± 20 and ± 30 mm Hg/ min. In the linear predictor of our control system, the threshold region was chosen to be ± 0.8 mm Hg through trial-and-error testing to obtain the best performance of the SFLC. We also replaced the SFLC by a normal FLC and a traditional PID controller under the same testing conditions for performance comparisons. In our simulations, the rate of the added disturbance to the variation of the MAP in each heartbeat was set at about 0.3 mm Hg.

Fig. 8 shows the control performance of the SFLC with a linear predictor, where the MAP is given at a changing rate of ± 20 mm Hg/min. The chamber pressure under the SFLC control as well as the desired MAP is shown in Fig. 8(a). It is observed that the chamber pressure follows the desired MAP closely. To see the control performance more closely, Fig. 8(b) shows the difference between the actual chamber pressure and the desired MAP and the SFLC output signals. It is found the tracking error was kept within a fixed amount when the MAP is ascending or descending. The SFLC output signals keep the pressure values positive in the ascending process and keep the pressure values negative in the descending process. The SFLC produces only small positive or negative output signals to keep the vessel volume at its maximum in the stabilizing state. Fig. 8(c) displays the amplitude of vessel volume pulse in each heartbeat. From this figure, we can find that the tracking error is about 2 mm Hg. Because the parameter σ in (7) is too large, the error of the normalized amplitude of vessel volume pulse is only about 10^{-3}. Therefore, if we can increase the resolution of the fuzzy term sets of $\overline{VOA}(n)$ and $\overline{VOA}(n-1)$, the tracking error is expected to be further reduced.

For performance comparison, in the second simulation we try to use a normal FLC to reach the optimal coupling condition. Since there is no model-based predictor and no subcontroller, the concept of "stochastic exploration" is applied here to design the fuzzy rules. In the beginning, the FLC guesses that the MAP has a descending changing tendency, so it decreases the tonometer's chamber slightly. If the guess is wrong (i.e., $\overline{VOA}(n)$ is further descending), the FLC will increase the chamber pressure again; otherwise, the FLC will keep the same control direction with faster speed, until $\overline{VOA}(n)$ gets close to the maximum. Therefore, the normal FLC designed here requires three input variables, including the current and preceding normalized oscillation amplitude of vessel volume, $\overline{VOA}(n)$ and $\overline{VOA}(n-1)$ and the amount of change in the chamber pressure, $CCP(n)$. The fuzzy term set for $CCP(n)$ is composed of nine membership functions: much push (MP), moderately push (DP), little push (LP), very little push (VLP), zero (Z), very little draw (VLD), little draw (LD), moderately draw (DD) and much draw (MD) and $\overline{VOA}(n)$ or $\overline{VOA}(n-1)$ is composed of five membership functions: BEST, BETTER, GOOD, WORSE and WORST, so there are 225 if-then rules totally. If the FLC guesses the tendency of MAP beginning to arise, $CCP(n)$ will not draw the chamber pressure. Thus, there are only the fuzzy terms MP, DP, LP, VLP, and Z that will be fired. When $\overline{VOA}(n)$ and $\overline{VOA}(n-1)$ fire the WORSE or WORST conditions, $CCP(n)$ will fire the MD or DD to compensate the chamber pressure. On the contrary, if the FLC guesses the tendency of MAP beginning to go down, $CCP(n)$ will not push the chamber pressure. Thus, there are only the fuzzy terms MD, DD, LD, VLD, and Z that will be fired. When $\overline{VOA}(n)$ and $\overline{VOA}(n-1)$ fire the WORSE or WORST conditions, $CCP(n)$ will fire the fuzzy terms MP or DP to compensate the chamber pressure. Therefore, there are only 124 if-then rules that will be used. The corresponding control performance of this simple FLC is shown in Fig. 9, where the stairwise outputs reflect the future of the exploration-typed control scheme. The curves in the figure obviously show that the controlled chamber pressure cannot stably and smoothly follow the desired MAP. Some previous papers [15], [37] also observed this phenomenon.

Finally, to compare the performance of the proposed scheme to that of a traditional approach, we replace the SFLC in Fig. 4 by a synthetic PID controller, which contains three PID subcontrollers and keep the other components in Fig. 4 unchanged. We have tried our best to tune each PID subcontroller to achieve its best performance and the simulation results are shown in

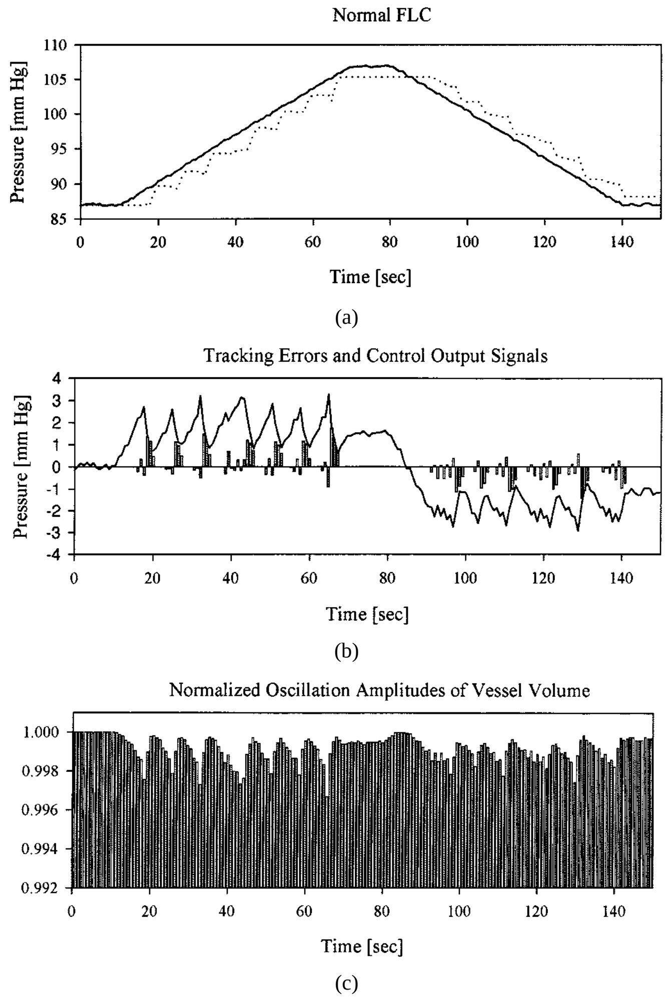

Fig. 9. Simulation results of the normal FLC for the MAP with a changing rate of ± 20 mm Hg/min. (a) The desired MAP (solid line) and the chamber pressure (CP) under control (dot line), (b) the difference between the desired MAP and the chamber pressure (solid line) and the FLCs output signals (bar lines), and (c) the normalized oscillation amplitude of vessel volume in each heartbeat.

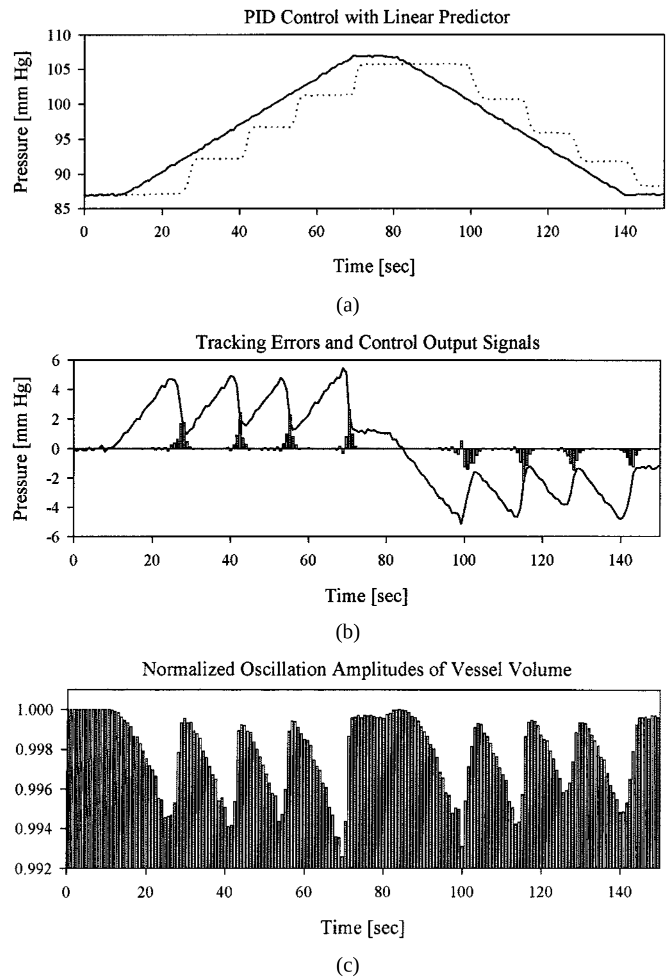

Fig. 10. Simulation results of the synthetic PID controller with a model-based linear predictor for the MAP with a changing rate of ± 20 mm Hg/min. (a) The desired MAP (solid line) and the chamber pressure (CP) under control (dot line), (b) the difference between the desired MAP and the chamber pressure (solid line) and the PID controller's output signals (bar lines), and (c) the normalized oscillation amplitude of vessel volume in each heartbeat.

Fig. 10. The results show that even with the model-based linear predictor, the PID-based control system cannot track the desired MAP accurately and stably. It was found in our simulation that the produced stairwise tracking errors were larger than those in Fig. 9. This is due mainly to the low tracking accuracy and speed of the PID controller, which in turn results in lower prediction accuracy of the linear predictor. Obviously, the lower prediction accuracy for the MAP will worsen the tracking accuracy of the PID controller. These two factors affect each other mutually. In fact, in our simulations, the synthetic PID controller usually failed to make the chamber pressure to follow the desired MAP at all; it took us a large number of trial-and-error design processes to obtain the synthetic PID controller producing the results in Fig. 10. The stairwise error oscillation phenomenon of the PID control was also found in [16], [22].

The results of our simulations are summarized in Table II. This table lists the maximum/minimum tracking errors and the mean square tracking errors (tracking MSE) of the three controllers mentioned above for three different changing rates of the MAP (± 10, ± 20 and ± 30 mm Hg/min). From the table, we see clearly that the SFLC with the model-based linear predictor

TABLE II
SUMMARY OF THE CONTROL PERFORMANCE OF VARIOUS CONTROLLERS IN THE PROPOSED MEASUREMENT SYSTEM

	SFLC with a model-based linear predictor			Normal FLC			PID controller with a model-based linear predictor		
Changing rate of MAP [mm Hg / min]	± 30	± 20	± 10	± 30	± 20	± 10	± 30	± 20	± 10
Max. Tracking Error [mm Hg]	2.6	2.4	2.0	3.6	3.3	2.8	6.7	5.5	4.6
Min. Tracking Error [mm Hg]	-3.0	-2.7	-1.9	-3.7	-2.9	-2.5	-5.5	-5.1	-4.4
Tracking MSE [mm Hg]	2.8	2.1	1.9	3.3	2.9	2.9	9.5	8.2	6.6

has the best performance among the compared counterparts for various changing rates of MAP.

V. CONCLUSIONS

This paper proposes the use of fuzzy logic control, called model-based synthetic fuzzy logic controller (SFLC), for achieving the optimal coupling condition in the noninvasive blood pressure measurement. A modified tonometer has been manufactured and used to successfully measure the continuous pressure waveform and the change in the arterial volume from nine subjects. By applying the curve-fitting technique on the experiment data, a Gaussian function was found and used to model the relationship of the oscillation amplitude of vessel volume to the transmural pressure. Based on this model, a linear predictor was set up to estimate the MAP trajectory in each heartbeat and the estimated results were feedback to the SFLC for choosing a proper subcontroller. The simulation results showed that the SFLC with three parallel subcontrollers and a model-based linear predictor was capable of precisely controlling the chamber pressure to tightly follow the time-varying MAP. In our comparison studies, we also observed that the SFLC with a model-based linear predictor had better performance than the normal FLC and the traditional PID controller. Since the whole control process is rather time efficient, the proposed control system can beat-to-beat control the chamber pressure in real time. Further clinical testing is required to verify these conclusions practically.

REFERENCES

[1] B. D. O. Anederson and J. B. Moore, *Optimal Control: Linear Quadratic Methods*. Englewood Cliffs, NJ: Prentice-Hall, 1989.

[2] P. D. Baker, D. R. Westenskow, and K. Kuck, "Theoretical analysis of noninvasive oscillometric maximum amplitude algorithm for estimating mean blood pressure," *Med. Biol. Eng. Comput.*, vol. 35, pp. 271–278, 1997.

[3] C. M. Buntin and F. H. Silver, "Noninvasive assessemnt of mechanical properties of peripheral arteries," *Ann. Biomed. Eng.*, vol. 18, pp. 549–566, 1990.

[4] C. R. Bussani and J. A. Mcewen, "Improved tracking of limb occlusion pressure for surgical tourniquets," *IEEE Trans. Biomed. Eng.*, vol. 35, pp. 221–229, 1988.

[5] E. Czogala and J. Leski, "On equivalence of approximate reasoning results using different interpretations of fuzzy if-then rules," *Fuzzy Sets Syst.*, vol. 117, pp. 279–296, 2001.

[6] G. Drzewiecki, V. Bansal, E. Karam, R. Hood, and H. Apple, "Mechanics of the occlusive arm cuff and its application as a volume sensor," *IEEE Trans. Biomed. Eng.*, vol. 40, pp. 704–708, 1993.

[7] G. Drzewiecki, R. Hood, and H. Apple, "Theory of the oscillometric maximum and the systolic and diastolic detection ratios," *Ann. Biomed. Eng.*, vol. 22, pp. 88–96, 1994.

[8] G. Drzewiecki, B. Solanki, J. J. Wang, and J. K. Li, "Noninvasive determination of arterial pressure and volume using tonometry," in *Proc. IEEE EMBS Conf.*, 1996, pp. 61–64.

[9] J. S. Eckerle, "Arterial tonometry," in *Encyclopedia of Medical Devices and Instrumentation*. New York: Wiley, 1988.

[10] F. K. Forster and D. Turney, "Oscillometric determination of diastolic, mean and systolic blood pressure—A numerical model," *ASME J. Biomech. Eng.*, vol. 108, pp. 359–364, 1986.

[11] L. A. Geddes, M. Voelz, C. Combs, D. Reiner, and C. F. Babbs, "Characterization of the oscillometric method for measuring indirect blood pressure," *Ann. Biomed. Eng.*, vol. 10, pp. 271–280, 1982.

[12] D. N. Ghista, G. Jayaraman, and H. Sandler, "Analysis for the transcutaneous continuous monitoring of arterial blood pressure," *Med. Biomed. Eng. Comput.*, vol. 16, pp. 715–726, 1978.

[13] H. H. Hardy and R. E. Collins, "On the pressure-volume relationship in circulatory elements," *Med. Biol. Eng. Comput.*, vol. 20, pp. 565–570, 1982.

[14] J. W. Huang and R. J. Roy, "Multiple-drug hemodynamic control using fuzzy decision theory," *IEEE Trans. Biomed. Eng.*, vol. 45, pp. 213–228, 1998.

[15] S. Isaka and A. V. Sebald, "An optimization approach for fuzzy controller design," *IEEE Trans. Syst., Man, Cybern.*, vol. 22, pp. 1469–1472, 1992.

[16] G. Jee and R. J. Roy, "Adaptive control of multiplexed closed-circuit anesthesia," *IEEE Trans. Biomed. Eng.*, vol. 39, pp. 1071–1080, Oct. 1992.

[17] R. Johansson, *System Modeling and Identification*. Englewood Cliffs, NJ: Prentice-Hall, 1993.

[18] J. H. Lai and C. T. Lin, "Application of neural fuzzy network to pyrometer correction and temperature control in rapid thermal processing," *IEEE Trans. Fuzzy Syst.*, vol. 7, pp. 160–175, Apr. 1999.

[19] C. T. Lin and C. S. G. Lee, *Neural Fuzzy Systems: A Neural-Fuzzy Synergism to Intelligent Systems*. Englewood Cliffs, NJ: Prentice-Hall, 1996.

[20] D. A. Linkens, J. S. Shieh, and J. E. Peacock, "Hierarchical fuzzy modeling for monitoring depth of anaesthesia," *Fuzzy Sets Syst.*, vol. 79, pp. 43–57, 1996.

[21] I. M. Iliev, "Improvements of noninvasive long-term blood pressure recording," *J. Clin. Eng.*, pp. 392–397, 1996.

[22] J. F. Martin, A. M. Schneider, M. L. Quinn, and N. T. Smith, "Improved safety and efficacy in adaptive control of arterial blood pressure through the use of a supervisor," *IEEE Trans. Biomed. Eng.*, vol. 39, pp. 381–388, Apr. 1992.

[23] G. W. Mauck, C. R. Smith, L. A. Geddes, and J. D. Bourland, "The meaning of the point of maximum oscillations in cuff pressure in the indirect measurement of blood pressure—Part II," *ASME J. Biomech. Eng.*, vol. 102, pp. 28–33, 1980.

[24] R. Raamat, J. Talts, K. Jagomagi, and E. Lansimies, "Methematical modeling of noninvasive oscillometric finger mean blood pressure measurement by maximum oscillation criterion," *Med. Biomed. Eng. Comput.*, vol. 37, pp. 784–788, 1999.

[25] R. P. Schnall, N. Gavriely, S. Lewkowicz, and Y. Palti, "A rapid noninvasive blood pressure measurement method for discrete value and full waveform determination," *Amer. Physiol. Soc.*, pp. 307–314, 1996.

[26] P. D. Stein and E. F. Blick, "Arterial tonometry for the atraumatic measurement of arterial blood pressure," *J. Appl. Physiol.*, vol. 30, pp. 593–596, 1971.

[27] S. Tanaka and K. Yamakoshi, "Ambulatory instrument for monitoring indirect beat-to-beat blood pressure in superficial temporal artery using volume-compensation method," *Med. Biol. Eng. Comput.*, vol. 34, pp. 441–447, 1996.

[28] M. Ursino and C. Cristalli, "Mathematical modeling of noninvasive blood pressure estimation techniques—Part I: Pressure transmission across the arm tissue," *ASME J. Biomech. Eng.*, vol. 117, pp. 107–116, 1995.

[29] ——, "A mathematical study of some biomechanical factors affecting the oscillometric blood pressure measurement," *IEEE Trans. Biomed. Eng.*, vol. 43, pp. 761–778, 1996.

[30] J. J. Wang, S. H. Liu, J. H. Hsieh, C. I. Chern, and C. Liu, "Fluctuation analysis of the continuous arterial blood pressue during Valsalva maneuver," *Biomed. Eng.: Applicat., Basis, Commun.*, vol. 11, pp. 59–66, 1999.

[31] L. X. Wang, *Adaptive Fuzzy Systems and Control: Design and Stablility Analysis*. Englewood Cliffs, NJ: Prentice-Hall, 1994.

[32] Y. Y. L. Wang, C. C. Chang, J. C. Chen, H. Hsiu, and W. K. Wang, "Pressure wave propagation in arteries: A model with radial dilatation for simulating the behavior of a real artery," *IEEE Eng. Med. Biol. Mag.*, vol. 16, pp. 51–54, Jan./Feb. 1997.

[33] B. M. Weiss, S. H. Rahmic, R. Rohling, and T. Pasch, "Radial artery tonometry: Moderately accurate but unpredictable technique of continuous noninvasive arterial pressure," *Bri. J. Anaes.*, vol. 76, pp. 404–411, 1996.

[34] K. Yamakoshi, A. Kamiya, H. Shimazu, H. Ito, and T. Togawa, "Noninvasive automatic monitoring of instantaneous arterial blood pressure using the vascular unloading technique," *Med. Biol. Eng. Comput.*, vol. 21, pp. 557–565, 1983.

[35] K. Yamakoshi, H. Shimazu, and A. Kamiya, "New oscillometric method for indirect measurement of systolic and mean arterial pressure in the human finger. Part 2: Correlation study," *Med. Biol. Eng. Comput.*, vol. 20, pp. 314–318, 1982.

[36] K. Yamakoshi, H. Shimazu, and T. Togawa, "Indirect measurement of instantaneous arterial blood pressure in the human finger by the vascular unloading technique," *IEEE Trans. Biomed. Eng.*, vol. BME-27, pp. 150–155, 1980.

[37] R. R. Yager and D. P. Filev, *Essentials of Fuzzy Modeling and Control*. New York: Wiley, 1994.

[38] H. Ying, M. Mceachern, D. W. Eddleman, and L. C. Sheppard, "Fuzzy control of mean arterial pressure in postsurgical patients with sodium nitroprusside infusion," *IEEE Trans. Biomed. Eng.*, vol. 39, pp. 1060–1070, 1992.

[39] P. Yong and L. A. Geddes, "A surrogate arm for evaluating the accuracy of instruments for indirect measurement of blood pressure," *Biomed. Instrum. Technol.*, vol. 24, pp. 130–135, 1990.

Jia-Jung Wang was born in Pingtung City, Taiwan, R.O.C., in 1962. He received the B.S. degree in 1985 and the M.S. degree in 1987 in biomedical engineering from Chung-Yuan University, Taiwan. He received the M.S. degree in 1995 and the Ph.D. degree in 1996 in biomedical engineering from Rutgers University, New Brunswick, NJ.

After serving two years of military service, he was with the National Science Council of the Republic of China as an Assistant Manager of the Division of Engineering Technology and Development from 1989 to 1992. He was the Chairman of the Department of Biomedical Engineering, Yuanpei Technical College, Taiwan, from 1996 to 2000. He is an Associate Professor with the Department of Biomedical Engineering, I-Shou University, Kaohsiung, Taiwan. His research interests include the design of biomedical instrumentation, analysis of hemodynamic signals and computer modeling of the cardiovascular system.

Dr. Wang was elected to the Phi Tau Phi Scholastic Honor Society in 1987. He is a member of the Chinese Biomedical Engineering Society.

Chin-Teng Lin (S'88–M'91–SM'99) received the B.S. degree in control engineering from National Chiao-Tung University, Hsinchu, Taiwan, R.O.C., in 1986 and the M.S.E.E. and Ph.D. degrees in electrical engineering from Purdue University, West Lafayette, IN, in 1989 and 1992, respectively.

Since August 1992, he has been with the College of Electrical Engineering and Computer Science, National Chiao-Tung University, where he is currently a Professor and Chairman of the Electrical and Control Engineering Department. He served as the Deputy Dean of the Research and Development Office of the National Chiao-Tung University from 1998 to 2000. His current research interests are fuzzy systems, neural networks, intelligent control, human–machine interface, image processing, pattern recognition, video and audio (speech) processing, and intelligent transportation system (ITS). He is the coauthor of *Neural Fuzzy System—A Neuro-Fuzzy Synergism to Intelligent System* (Englewood Cliffs, NJ: Prentice-Hall, 1996) and author of *Neural Fuzzy Control Systems with Structure and Parameter Learning* (Singapore: World Scientific, 1994). He has published more than 60 journal papers in the areas of soft computing, neural networks, and fuzzy systems, including about 40 IEEE TRANSACTIONS papers. He is an Associate Editor for the *Journal of Automatica*.

Dr. Lin is a member of Tau Beta Pi and Eta Kappa Nu. He is also a member of the IEEE Computer Society, the IEEE Robotics and Automation Society, and the IEEE Systems, Man, and Cybernetics Society. He has been the Executive Council Member of the Chinese Automation Association since 1998. He has been the Chairman of the IEEE Robotics and Automation Society, Taipei Chapter, since 2000 and an Associate Editor of the IEEE TRANSACTIONS ON SYSTEMS, MAN, AND CYBERNETICS—PART B since 2001. He won the Outstanding Research Award granted by National Science Council (NSC), Taiwan, from 1997 to 2001, the Outstanding Electrical Engineering Professor Award granted by the Chinese Institute of Electrical Engineering (CIEE) in 1997, and the Outstanding Engineering Professor Award granted by the Chinese Institute of Engineering (CIE) in 2000. He was also elected to be one of the 38 Ten Outstanding Young Persons in Taiwan in 2000.

Shing-Hong Liu received the B.S. degree in electronic engineering from the Feng-Jia University, Taizhon, Taiwan, R.O.C., in 1990 and the M.S. degree in biomedical engineering from the Cheng Kung University, Tainan, Taiwan, in 1992. He is currently pursuing the Ph.D. degree in the Department of Electrical and Control Engineering, National Chiao-Tung University, Hsinchu, Taiwan.

Since August 1994, he has been a Lecturer with the Department of Biomedical Engineering, Yuanpei Institute of Science and Technology, Hsinchu. His current research interests are digital signal processing, fuzzy control, and designing biomedical instruments.

Zu-Chi Wen received the M.D. degree from the Taipei Medical University, Taipei, Taiwan, R.O.C. in 1990.

From 1990 to 1994, he was a Resident Doctor with the Internal Department of Provincial Hsinchu Hospital, Hsinchu, Taiwan. From 1994 to 1996, he was a Cardiac Research Fellow with the Veteran General Hospital, Taipei. He had been an Attending Doctor with the Hsinchu Hospital, Department of Health since 1996 and has served as the Chief of the Cardiac Department since 2000. His current research interests are autonomic control of heart and vascular angioplasty. He has published over 50 journal papers in the areas of arrhythmia and autonomic control of heart.

Dr. Wen is a member of the Taiwan Society of Cardiology and the Taiwan Society of Internal Medicine and Critical Care Medicine. He won the outstanding Young Investigator Award granted by Taiwan Society of Cardiology in 1999.